University of Huddersfield

University of Huddersfield Repository

Elliott, Paul I.

New cyclometalated iridium(III) dye chromophore complexes for n-type dye-sensitised solar cells

Original Citation

Elliott, Paul I. (2017) New cyclometalated iridium(III) dye chromophore complexes for n-type dye-sensitised solar cells. Inorganica Chimica Acta, 457. pp. 81-89. ISSN 0020-1693

This version is available at https://eprints.hud.ac.uk/id/eprint/30721/

The University Repository is a digital collection of the research output of the University, available on Open Access. Copyright and Moral Rights for the items on this site are retained by the individual author and/or other copyright owners. Users may access full items free of charge; copies of full text items generally can be reproduced, displayed or performed and given to third parties in any format or medium for personal research or study, educational or not-for-profit purposes without prior permission or charge, provided:

- The authors, title and full bibliographic details is credited in any copy;
- A hyperlink and/or URL is included for the original metadata page; and
- The content is not changed in any way.

For more information, including our policy and submission procedure, please contact the Repository Team at: E.mailbox@hud.ac.uk.

http://eprints.hud.ac.uk/

New cyclometalated iridium(III) dye chromophore complexes for n-type dye-sensitised solar cells

Alessandro Sinopoli,[a] Christopher J. Wood,[b] Elizabeth A. Gibson*[b] and Paul I. P. Elliott*[a]

a Department of Chemistry, University of Huddersfield, Queensgate, Huddersfield, HD1 3DH, UK

b School of Chemistry, Newcastle University, Newcastle, NE1 7RU, UK

* corresponding authors: elizabeth.gibson@ncl.ac.uk; p.i.elliott@hud.ac.uk

Abstract. The synthesis of seven iridium complexes where aryl-1,2,3-triazole (Ar-tz) ligands act as cyclometalating ligands and 2,2'-bipyridyl-4,4'-dicarboxylic acid (dcb) as N^N ancillary/anchoring ligand, is described. The new dye complexes $[Ir(Ar\text{-}tz)_2(dcb)][PF_6]$ (**AS1-7**) were prepared in a two stage procedure with iridium-chloride dimer isolation. DFT analysis together with photophysical investigations reveal how using different substituents on the phenyl ring, or a different aryl system, lead to the tuning of the absorption and emission properties of these complexes. Computational studies therefore demonstrate an ideal HOMO-LUMO directionality for the $[Ir(Ar\text{-}tz)_2(dcb)]^+$ framework, promoting a favourable electron transfer into the TiO_2 conduction band upon photoexcitation. Preliminary unoptimized tests on TiO_2 DSSCs have been carried out which show similar photovoltaic performance to their $[Ir(ppy)_2(dcb)][PF_6]$ (ppy = 2-phenylpyridine) benchmark.

Keywords. *DSSC; Cyclometalated Iridium(III) complexes; sensitizers; triazole.*

1. Introduction

The development of high efficiency dye-sensitised solar cells (DSSCs) has been dominated by ruthenium(II)-based complexes with famous example being the archetypal **N3** $[Ru(dcb)_2(NCS)_2]$. [1, 2] The success of these dye systems stems from their favourable electrochemical properties and reasonably strong MLCT/LLCT-based bands in their optical absorption spectra. Much of this work has focussed upon modification of the archetypal **N3** dye structure, by replacement of one of the dcb ligands with a 2,2'-bipyridyl ligand appended with auxiliary chromophore and/or electron donor

functionalities. [3-8] Other efforts have focussed on the replacement of the monodentate thiocyanate ligand that are susceptible to ligand substitution by anionic chelate ligand including pyridylpyrazolates and cyclometalated arylpyridines. [8-10] This lead to increases stability and durability of the resultant dyes and can also enable greater scope and more efficient tuning of optical and electronic properties.

Other d^6 metal complex systems have been explored including cyclometalated iridium(III) systems. [11-16] Heteroleptic biscyclometalated iridium(III) complexes typically display intense phosphorescent emission and have therefore seen widespread utilisation in light-emitting electrochemical cells. [17-20] Their use as sensitisers in DSSC is on the other hand limited, amongst the first examples of these complexes to be applied in DSSC includes $[Ir(ppy)_2(dcb)]^+$ (ppyH = 2-phenylpyridine). [16] This complex, and analogues of it, exhibits much poorer DSSC efficiencies than their ruthenium counterparts, however, stemming largely from a much reduced optical absorption cross-section. However, cyclometalated iridium(III) complexes do have some significant advantages over traditional ruthenium dyes that allow ample room for further dye development and the improvement of their optical properties. The highest occupied molecular orbital (HOMO) in complexes of this type have metallic d-orbital character with a significant contribution from the π-system of the metalated aryl rings whilst the lowest unoccupied molecular orbital (LUMO) is localised on the electrode anchoring dcb ligand. Variation of the aryl substituents therefore leads to facile tuning of the electronic properties and optical absorption properties of the resultant dyes. [21-23] Further, the stereochemistry of biscyclometalated heteroleptic iridium complexes is highly selective meaning that the charge transfer directionality characteristics can be confidently predicted. Thus, with the anchoring carboxylate moieties localised on the ‘acceptor’ dcb ligand and the ‘donor’ aryl ring of the cyclometalated ligand lying on the opposing side of the complex the charge transfer directionality is therefore supremely organised for favourable charge injection into the TiO_2-based anode when incorporated in an n-type DSSC (Figure 1).

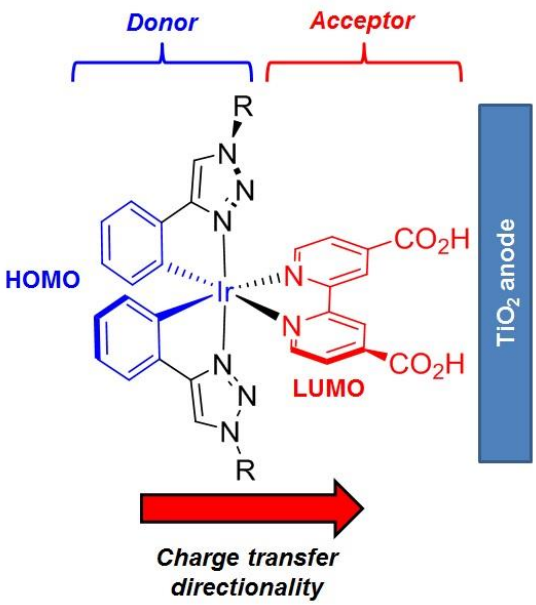

Figure 1. General structure and conceptual design of iridium(III) aryltriazole-based DSSC dyes.

In the context of the experimental studies detailed herein, the use of copper-catalysed alkyne/azide cycloaddition offer further advantages [24, 25]; unoccupied orbitals localised on the resultant triazole moiety of the cyclometalated ligands are much higher in energy than those of the archetypal ppy-based ligand thus eliminating competition for the localisation of the LUMO of complex ensuring that it is dominated by the dcb ligand. [21, 26] This destabilisation relative to ppy-based ligands also results in a destabilising perturbation of orbital localised on the aryl ring thus leading to a higher energy HOMO for the resultant complexes and therefore a potentially red-shift absorption spectrum and more efficient light harvesting. The versatility of the copper-catalysed alkyne/azide cycloaddition CuAAC route and the ready availability of alkyne starting materials (or facile routes to their synthesis) enables enormous scope for electronic and spectroscopic tuning and for the incorporation into the cyclometalated ligand precursor of ancillary electron donor groups and chromophores. [27]

In the current contribution, we there present our preliminary proof of principle results on a series of simple biscyclometalated aryltriazole complexes and their utilisation in test n-type DSSC devices.

2. Materials and methods

Chemicals were purchased from Aldrich and Acros, iridium was purchased from Precious Metal Online (Australia) and used as received. All complexation reactions were carried out under nitrogen. $[Ir(ppy)_2(dcb)][PF_6]$ [16] (**2.1**), 4,4'-Dicarboxy-2,2'-Bipyridine (dcb) [28] and Bestmann-Ohira reagent [29] were all prepared according to literature procedures. ^{1}H NMR and ^{13}C NMR spectra were recorded on a Bruker Advance 400 MHz instrument. Mass spectrometry data were collected on a Bruker Micro Q-TOF instrument. UV-Visible absorption spectra were recorded on a Varian Cary 300 spectrophotometer and corrected emission spectra were recorded on a Horiba Fluoromax-4 spectrofluorometer.

2.1. Dye sensitised solar cell fabrication

FTO glass was used as current collector (TCO30-8, 3 mm thick glass substrate with a 8 Ω/sq). Cleaned and dried FTO electrodes were immersed into a 40 mM aqueous $TiCl_4$ solution at 70 °C for 30 minutes and washed with pure water and ethanol and dried. Then the plates were cleaned in a boiling acetone bath for 15 minutes. A layer of nanocrystalline TiO_2 paste (Solaronix Ti-Nanoxide D) was coated on the FTO glass plates by doctor blade technique, using a round mask (5 mm diameter, 0.2 cm^2 area) made by adhesive tape (3M Magic). The film was dried for 5 minutes on a hotplate and a second layer of TiO_2 was deposited as before. The films were sintered at 450 °C for 30 minutes. After cooling to 80 °C, the TiO_2 electrodes were immersed into a 0.5 mM dye solution in a mixture of ethanol/tert-butanol 4:1 and kept at 45 °C overnight in the dark.

The Pt catalyst was deposited on the FTO glass, coating with 10 µL cm^{-2} of H_2PtCl_6 solution (5 mM isopropanol solution), air dried and heated at 400 °C for 15 minutes. The dye-covered TiO_2 electrodes, previously washed with acetonitrile, and Pt-counter electrodes were assembled into a sandwich-type cell and sealed with a Surlyn hot-melt gasket of 60 µm thickness. A solution of 0.4 M 1-butyl-3-methyl-imidazolium iodide, 0.03 M I_2 and 0.3 M LiI in acetonitrile:valeronitrile 9:1, was used as electrolyte. The edges of the FTO were painted with a silver conductive painting.

2.2. Computational methods

DFT calculations were carried out using the NWChem 6.0 and 6.1 software package. [30] Calculations were carried out using the B3LYP hybrid functional (20% Hartree–Fock), [31] Stuttgart relativistic small core ECP [32] for iridium and 6-311G* basis sets for all other atoms. Molecular structures and molecular orbitals were visualized using the ccp1 graphical user interface. The ground state geometries of all complexes were first optimized and molecular orbital energies determined. TD-DFT calculations were then used at the ground state geometries to derive vertical excitation energies and hence simulated absorption spectra. TD-DFT calculations on optimised structures in CH_3CN by using the COSMO solvation model [33] built in NWChem software were used to obtain the electronic spectra and molecular orbital energy levels. The benzyl (-CH_2-Ph) groups and the propyl groups have been approximated to methyl groups in order to simplify the calculations, for this reason complexes **AS3** and **AS7** are represented and calculated using the same geometry.

3. Results & Discussion

A range of aryl triazole ligand precursors were made by both CuACC and Bestmann-Ohira B.O. reactions. Most of the ligands shown below were synthesised using a slightly modified version of a pre-existing method (Route B, Table 1), [29] while the B.O. reagent itself was prepared from dimethyl 2-oxopropylphosphonate. The rest of the aryl-ligands were synthesised by the alkyne route (Route A, Table 1).

Table 1. Summary of synthetic routes to aryltriazole ligand precursors.

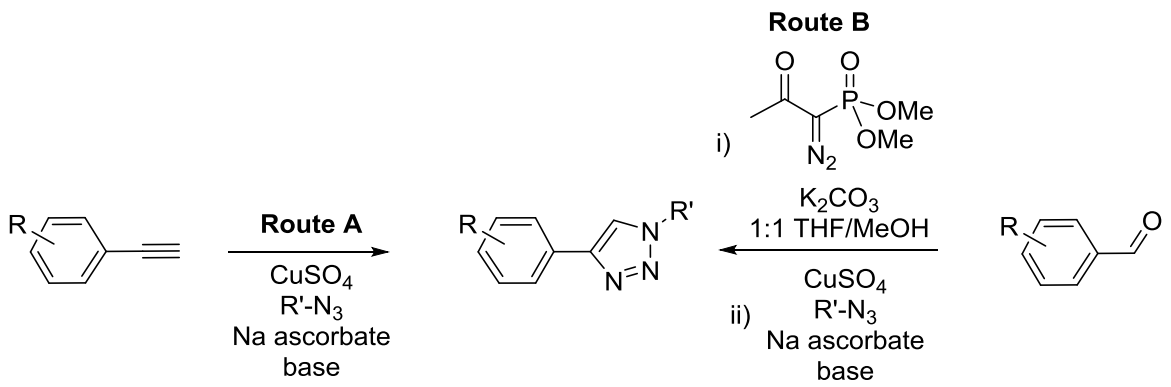

Ligand	Aryl synthon	Route	Aryltriazole product	Yield / %

a	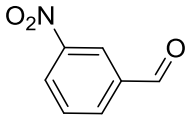	B	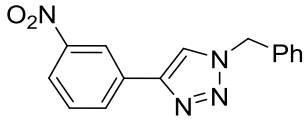	85
b	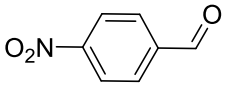	B	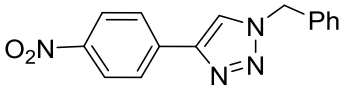	94
c	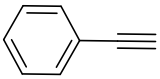	A	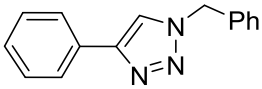	45
d	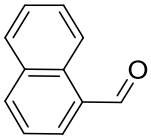	B	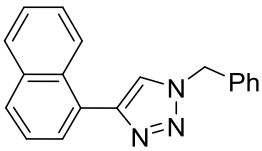	75
e	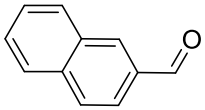	B	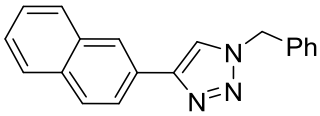	58
f	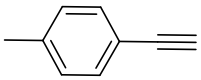	A	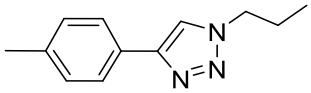	64
g	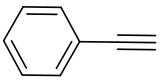	A	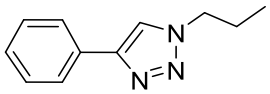	71

Ligands **a-b** and **d-e** where prepared in a one-pot B.O. synthetic procedure (Route B, Table 1) starting from the corresponding aldehydes. The starting alkynes were prepared *in situ* from corresponding aldehydes by reaction with B.O. reagent, in presence of K_2CO_3, in THF/MeOH mixture at room temperature for 24 hours. Upon completion of the alkyne formation, the pre-isolated benzylazide was added in the presence of a catalytic quantity of $CuSO_4$ and sodium ascorbate, stirring at room temperature for further 24 hours. The products were isolated by water/EtOAc extraction and then purified by column chromatography.

Ligand **c** was prepared from isolated benzyl azide (Route A, Table 1). The latter was prepared by reaction of benzyl bromide with an excess of sodium azide in dimethylsulfoxide. Upon completion, the reaction was quenched with water, and the azide extracted into diethyl ether. Benzyl azide was stored at -4°C and used in subsequent reactions. The benzyl triazole was formed by reaction of the azide with an excess of phenyl acetylene in the presence of one equivalent of $CuSO_4$ and two equivalents of sodium ascorbate in THF and water. After stirring at room temperature for 30 minutes, isolation of the product was achieved by partitioning between dichloromethane and aqueous ammonia

to remove copper. Purification of the ligand was achieved by recrystallization from dichloromethane and hexane.

Ligands **f-g** where prepared in a one-pot CuAAC synthetic procedure (Route A, Table 1) starting from the corresponding propyl halide and alkyne. The starting propyl azide was prepared *in situ* from corresponding propyl bromide by nucleophilic substitution with a slight excess of sodium azide stirring in dimethylsulfoxide at room temperature for 2 hours. Upon completion of the substitution reaction, the remainder of the starting material required for the CuAAC was added to the reaction; a slight excess of the alkyne was added in the presence of a catalytic quantity of $CuSO_4$, sodium ascorbate and 2,6-lutidine. The products were isolated by simple filtration of the reaction mixture and were further purified by recrystallization from dichloromethane and hexane. All ligands were isolated in moderate to good yields

Ligands **a-g** have been fully characterised using ^{1}H and ^{13}C NMR spectroscopy and mass spectrometry. The ^{1}H NMR spectra for the free ligands show a distinct diagnostic signal for the C-H proton of the triazole ring. These appear as singlet resonances over the range of δ 7.5-8.6. These signals show nOe interactions in their two dimensional NOESY spectra with the ortho-protons of the 4-aryl substituent and the α-protons of the 1-alkyl group or 1-benzyl group, therefore confirming the 1,4-regiochemistry of the 1,2,3-triazole. Successful synthesis of **a-g** was also confirmed using FT-IR spectroscopy where the lack of the azide and acetylene stretching modes at around 2100 to 2150 cm^{-1} indicated that no starting materials were present and that the reactions had gone to completion.

All the tabled ligands prepared by a tandem Bestmann-Ohira/‘Click’ coupling and standard CuAAC (Table 1) have been used to realize biscyclometalated complexes (Scheme 1). As shown in scheme 1 the standard synthesis of cyclometalated iridium complexes are based upon the formation of the iridium (III) chlorobridged dimer. Typically, $IrCl_3 \cdot 3H_2O$ was dissolved in 2-ethoxyethanol:H_2O (3:1) and the solution was degassed with nitrogen at 80 °C for 20 minutes, then 2 equivalents of cyclometalating ligand (Table 1) was added and the mixture heated to reflux at 125 °C for 6 hours.

The crude dimer was filtered under vacuum and recrystallized from DCM/hexane. The solid was used without any further purification

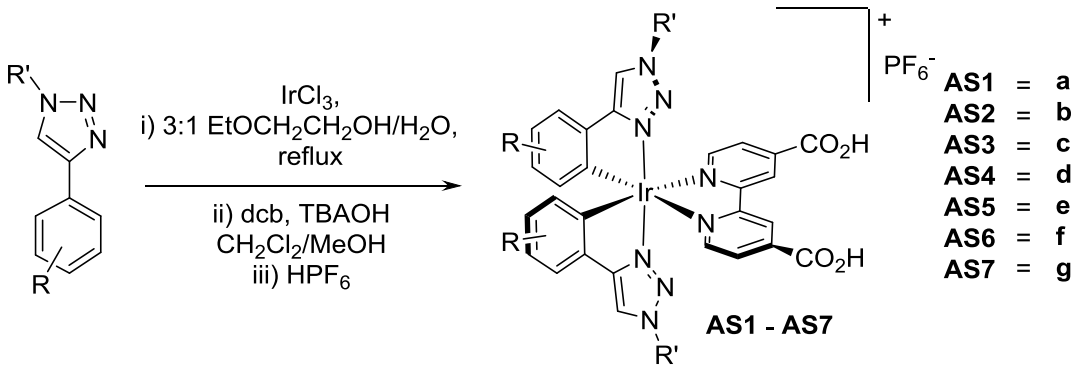

Scheme 1. Synthesis of dye complexes **AS1**-**AS7** (TBAOH = tetrabutylammonium hydroxide).

For the preparation of the final complexes, a solution of 2,2'-bipyridine-4,4'-dicarboxylic acid and TBAOH 1M in methanol was added to a solution of chloro-bridged dimer complex in a mixture of CH_2Cl_2-MeOH (2:1 v/v) and heated at reflux under a nitrogen atmosphere (Scheme 1). After 6 hours, the solution was cooled to room temperature. The solution was evaporated to dryness under reduced pressure and the solid was dissolved in a minimal amount of methanol and HPF_6 was added to precipitate the product. The solution was concentrated to induce further crystallisation and the solid was filtered over a porous glass frit, washed with water and ether and then dried. The product was purified by column chromatography on silica to provide the desired product. The products were recrystallized from acetonitrile and ether to yield from yellow to red solids in modest yields. The complexes [Ir(dcb)(**a-g**)$_2$][PF_6] (**AS1-7**) have been fully characterised using ^{1}H and ^{13}C NMR spectroscopy and mass spectrometry. The complex [Ir(dcb)(ppy)$_2$][PF_6] (**2.1**) was prepared for comparison.

The ^{1}H NMR spectra for complexes **AS1-7** show 3 signals between 8-10 ppm, for the coordinated 4,4'-substituted-bipyridine (♦ Figure 2) and a distinct diagnostic signal for the C-H proton of the triazole ring (▼ Figure 2). This appears as singlet resonances over the range of ppm 7.5-8.6. The metalated aryl rings showed a single set of resonances as consequence of the C_2 symmetry of the

$Ir(C^N)_2$ fragment, the number of signals is reduced by one (in comparison with the free ligand) due to the metalation (▲ Figure 2).

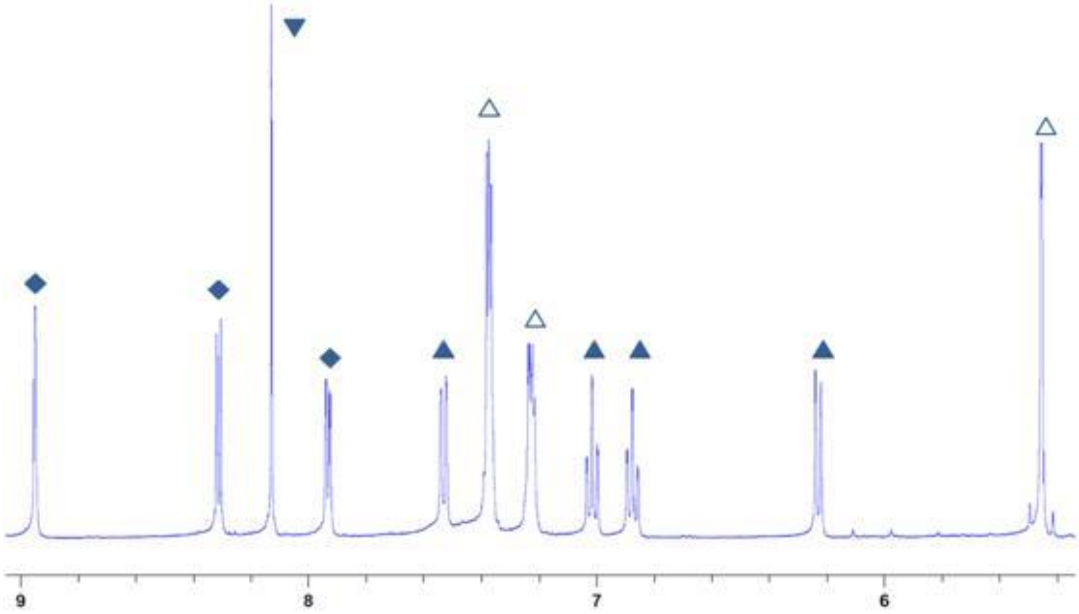

Figure 2 Aromatic region of the ^1H NMR spectrum of complex **AS3** (CD_3CN). ▼ proton of the triazole ring; ♦ protons of the dcb ligand; ▲ protons of phenyl cyclometalated ring; Δ protons of the benzyl fragment.

The use of different aryl fragments led to a good tunability of the HOMO energy, affecting the electronic properties of the final iridium complexes. Also, the combination of the high energy triazole π system with the electron withdrawing dcb ligand leads to an optimal HOMO-LUMO directionality.

UV-Visible absorption spectra of complexes **AS1-7** along with those of $[Ir(dcbpy)(ppy)_2][PF_6]$ were recorded in aerated acetonitrile and are showed in Figure 3. Photophysical data are summarised in Table 2.

The absorption spectra of these compounds are typical of the iridium complexes. They show intense bands in the ultraviolet region between 200 and 300 nm. These bands are attributed to spin-allowed π-π* ligand-centred (LC) transitions. These assignments were made on assessment of closely related metal complexes in the literature. [34-36] The less intense, lower energy absorption features from 300 to 600 nm are due to charge-transfer (CT) transition. Two types of CT transitions can be distinguished

in the spectra: bands of moderate intensity between 300 and 400 nm may be assigned to MLCT overlapping with LLCT transitions; and transitions with much weaker intensity at longer wavelengths are tentatively assigned to ^{3}MLCT. [37] These assignments are confirmed by an analysis of the typology of the orbitals implied in the major TD-DFT transitions.

Looking at the values reported in Table 2, the complexes with electrowithdrawing group (**AS1-2**) show a blue-shifted profile, consistent with the stabilization of their HOMO energy (fig).

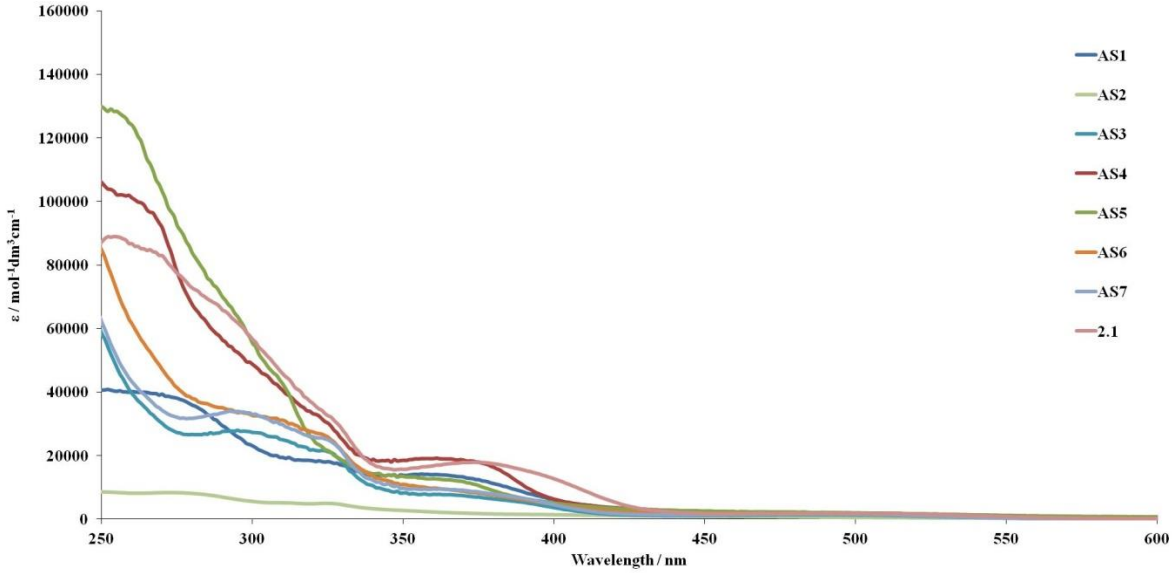

Figure 3. Absorption spectra for **AS1-7** dyes in acetonitrile.

Table 2 Summarised photophysical absorption and emission data for complexes **AS1-7**.

Dye	λ_{max}^{abs} / nm (ε / mol^{-1}dm^{3}cm^{-1})	λ_{max}^{em} / nm
AS1	222 (48515), 265 (39888), 322 (18388), 361 (14168) 467 (1326)	554
AS2	266 (6175), 405 (507)	568
AS3	234 (80103), 293 (27775), 365 (7770), 483 (1399)	647
AS4	238 (123073), 259 (101194), 362 (19066), 494 (2059)	671
AS5	246 (130496), 354 (13268), 484 (2163)	661

AS6	225 (118523), 302 (32537), 367 (9108), 478 (1774)	647
AS7	222 (109381), 294 (33800), 370 (9200), 495 (1620)	647
2.1	253 (88830), 372 (17866), 507 (1794)	601

As shown in Figure 3, the absorption coefficients of these dyes, in the visible range, are below 2000 $M^{-1}cm^{-1}$. These values unfortunately confirm the light harvesting limits of cyclometalated iridium complexes. However, the chromatic tunability, gained by the use of different phenyl-triazole ligands, looks remarkable

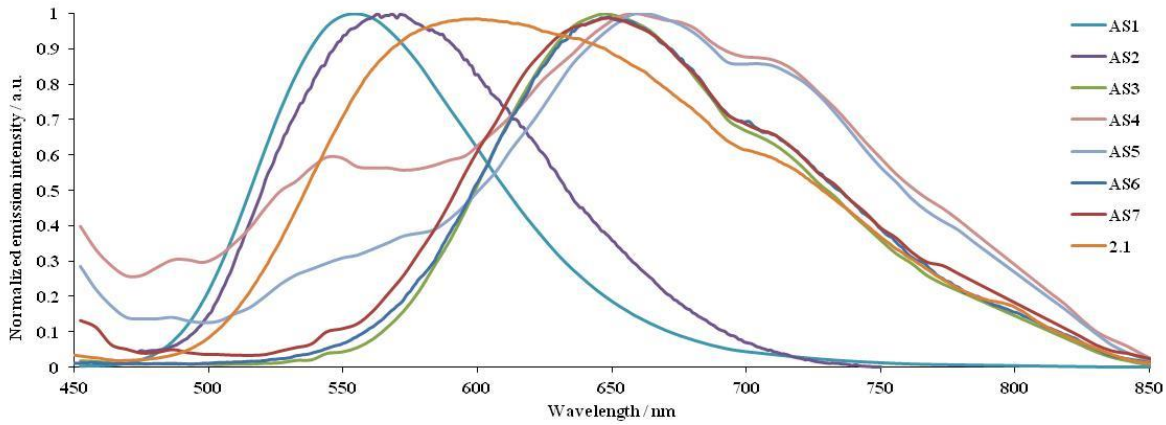

Figure 4. Normalised emission spectra for the eight aryl-triazole complexes **AS1-7** in aerated acetonitrile (excited at 400nm).

All complexes were found to emit in acetonitrile solutions at room temperature and the emission spectra are shown in Figure 4. The emission maxima for complexes **AS1-2** are around 560 nm, blue shifted relative to the other complexes, due to the electrowithdrawing effect of nitro groups leading to a HOMO energy stabilization, consistent with the UV-Vis absorption trend. [34] These bands are assigned to phosphorescent emission from triplet metal-to-ligand charge-transfer (^{3}MLCT) excited states. Complexes **AS3-7** show a similar emission profiles with maxima around 660 nm, demonstrating how the electron donating methyl and larger naphthyl π system don't have that much tuning effect. For this last group, the PL spectra possibly display vibronic-structured emission bands, whereas for the remaining two species, the vibronic structure, although still present, is less evident.

In the designed n-type dyes, the LUMO distribution is well located along π system of the dcb ligand involving the nitrogen, the carbon and partially the oxygen atoms. The iridium d-orbitals together with the phenyl ring orbitals of the triazole ligands, contribute to the HOMO density. The LUMO localised on the anchoring ligand, makes the electronic distribution on these complexes, ideal for their electron injection on titanium oxide. On the other side, the HOMO localised away from the carboxylic groups will avoid the electron-hole recombination. The frontier orbitals are collocated in Figure 7 for the seven investigated compounds plus complex **2.1** as reference. The benzyl groups and the propyl groups have been approximated to methyl groups in order to simplify the calculations, for this reason complexes **AS3** and **AS7** are represented and calculated using the same geometry.

Table 3 HOMO and LUMO energy values

Dye	HOMO / eV	LUMO / eV	Δ / eV
AS1	-6.51	-3.25	3.26
AS2	-6.43	-3.23	3.21
AS3	-5.86	-3.12	2.74
AS4	-5.73	-3.17	2.55
AS5	-5.72	-3.14	2.59
AS6	-5.79	-3.12	2.68
2.1	-5.94	-3.25	2.69

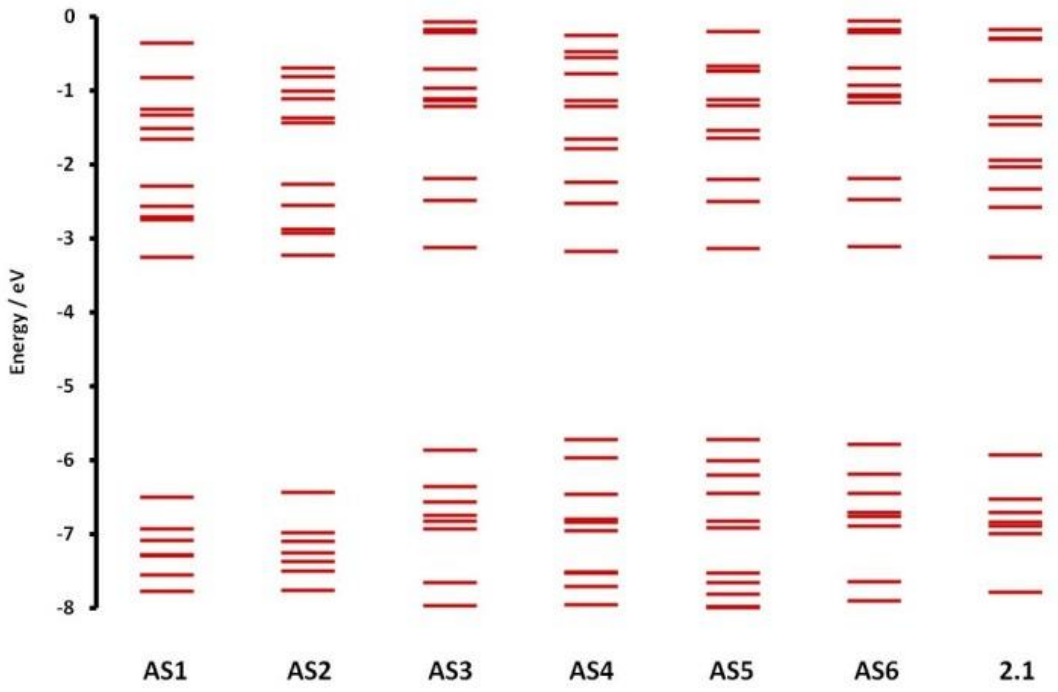

Figure 5. Energy level diagram for the frontier molecular orbitals of the complexes **AS1-6** plus **2.1**.

The calculated energy levels of **AS1-7** complexes showed as the LUMO level value is about -3.2 eV without any significant change across the series as expected. This is due to the coordination of the same dcb ancillary ligand. The HOMO energies lie between -5.94 and -5.71 eV except for complexes **AS1-2**, which include a nitro group on the phenyl ring, underlining its electron withdrawing effect. In fact, those two complexes show a substantial stabilization of their HOMO energies compared with **2.1** benchmark, whereas the HOMO energies of complexes **AS3-7**, containing phenyl and naphthyl fragments, look slightly destabilized.

For an electron injection probability from the sensitizer excited-state into the conduction band of TiO_2, an optimal effect is reached when the relevant virtual orbital of the dye significantly extends on the anchoring groups in order to mix with the conduction band wave function of the semiconductor. The degree of mixing can be estimated to a first extent from the size of the molecular orbitals on the binding groups. Conversely, the back charge recombination reaction will be slow if the hole (on the oxidised dye) lies far away from the injected electron, which is localized on the semiconductor. This condition is respected when the implied occupied orbitals (typically the HOMO) are remote from the anchoring groups.

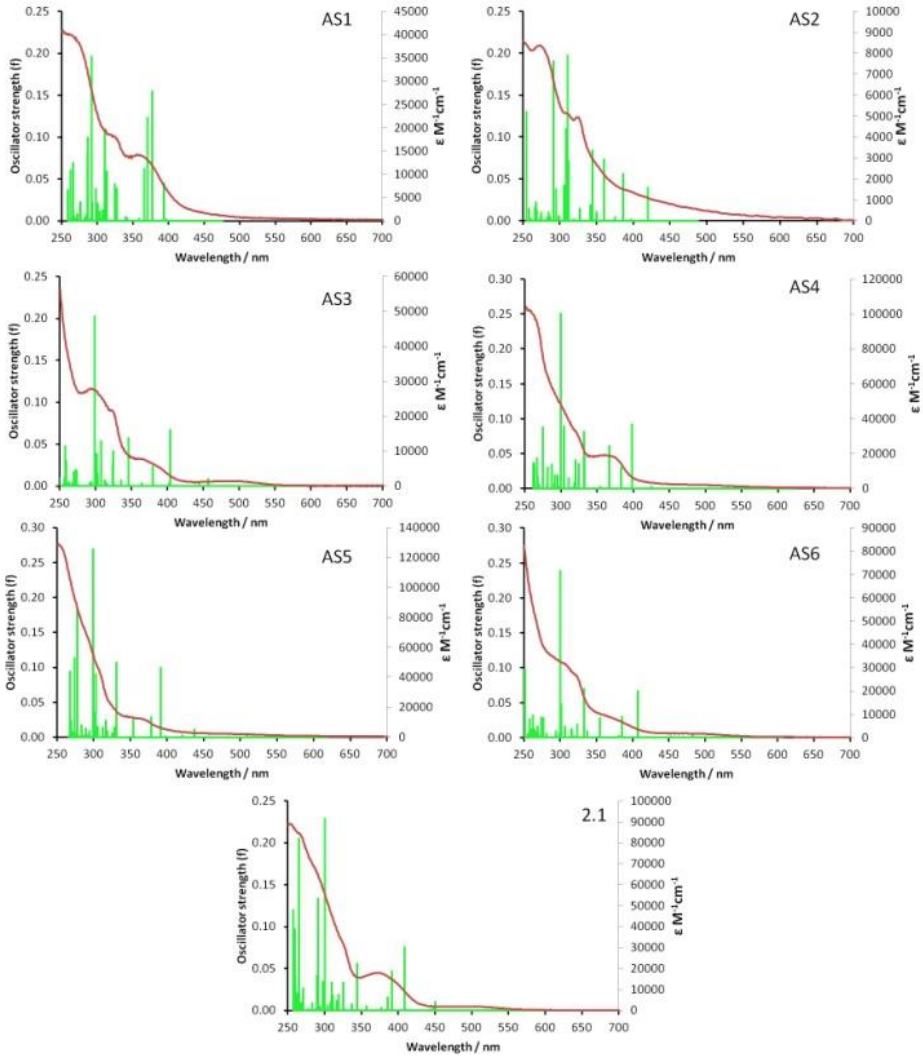

Figure 6. TDDFT calculated absorption spectra (green lines) for complexes **AS1-6** and **2.1** with experimental spectra (red trace) overlaid.

Time-dependent DFT (TD-DFT) calculations were carried out on the optimised geometries of each complex in order to determine vertical excitation energies. Simulated absorption spectra overlaid with experimental spectra are shown in Figure 6.

The excitations to the S_1 state all complexes are primarily HOMO→LUMO in character, however, they are of low oscillator strength and will therefore contribute little to the absorption spectra (see SI). The major transitions observed for all complexes between 350 and 450 nm are primarily of ^{1}MLCT

character. This outcome is consistent with the band observed experimentally (Figure 3). From TDDFT analysis, the predicted transitions correlate well with the experimental spectra.

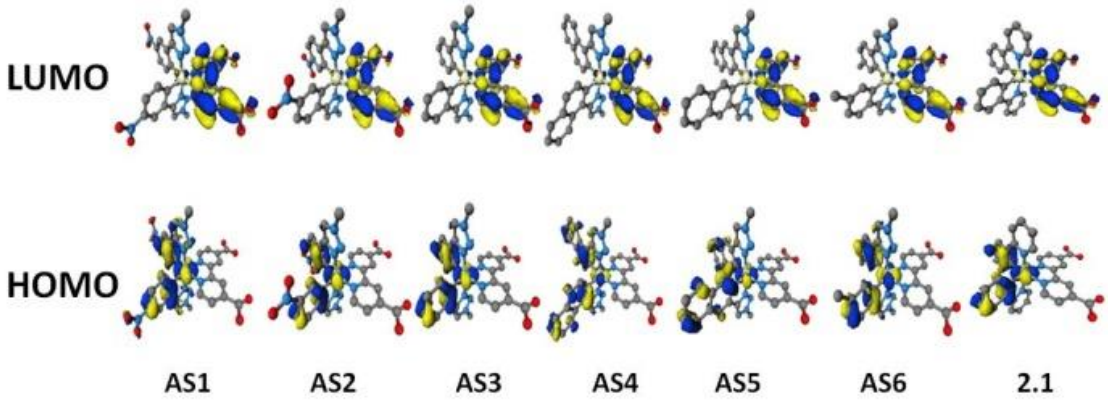

Figure 7. Optimised ground state geometries for complexes **AS1-6**, **2.1**, HOMO density on the bottom, LUMO on the top

All the complexes presented, they all have a transition in common in the range of 290-311 nm, always with oscillator strength higher than 0.20 resulting like the most probable transition and assigned as a mixture of MLCT/LC in character. Together with this main transition, complexes **AS3-6** show also a significant peak across 400nm with a strong MLCT/LLCT character (see SI). The transitions for complexes **AS1-2** look more structured. (see SI).

Sandwich-type solar cells were assembled using **AS1-7** sensitised nanocrystalline TiO_2 as the working electrodes, platinised conducting glass as the counter electrode and iodide/triiodide in acetonitrile as electrolyte. The photovoltaic performances of solar cells based on these iridium complexes **AS1-7** and **2.1**, as benchmark sensitizer, are summarised in Table 3. Figure 8 shows the current–voltage characteristics of the dyes under AM 1.5.

Table 3 Photovoltaic parameters of tested dyes.

DYE[a]	J_{SC} / mA cm^{-2}	V_{OC} / V	FF	η / %
AS1	1.41	0.434	0.69	0.42
AS2	0.92	0.423	0.63	0.24
AS4	0.985	0.491	0.65	0.31

AS5	0.634	0.489	0.66	0.2
AS6	2.405	0.433	0.6	0.62
AS7	1.15	0.403	0.64	0.3
2.1	1.1	0.551	0.59	0.35

[a] ***AS3*** *dye has been not tested because of its similarity with* ***AS7****.*

The overall conversion efficiencies η were derived from the equation: $\eta = J_{sc} \times V_{oc} \times FF$, where J_{sc} is the short circuit current density, V_{oc} the open circuit voltage, and FF the fill factor.

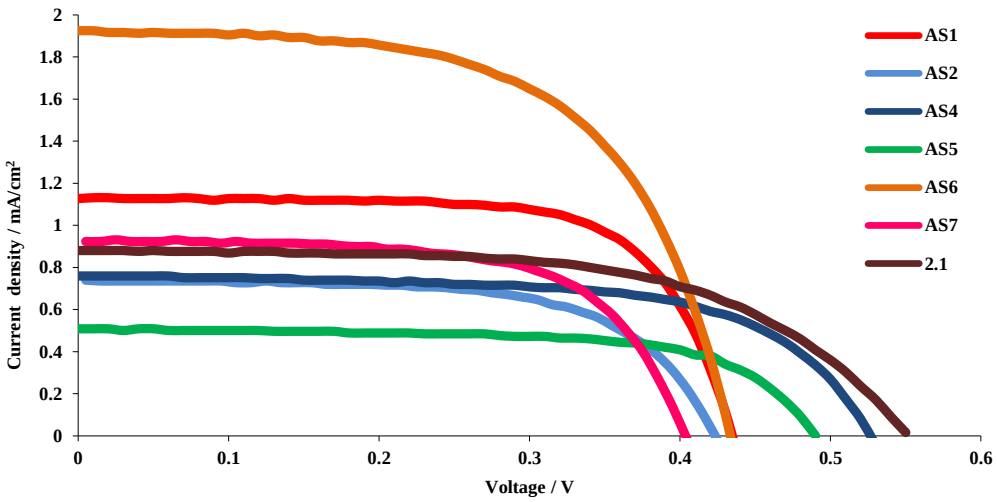

Figure 8 Current-Voltage curves DSSC constructed using iridium complexes **AS1-7, 2.1**

The obtained photovoltaic efficiencies for the tested dyes were generally low, this is not unexpected and attributable to their blue-shifted absorption profiles in their absorption spectra which would result in lesser light harvesting efficiency. The best result is reached by complex **AS7** with an efficiency of 0.62%, nearly double compared to $[Ir(dcb)(ppy)_2][PF_6]$ benchmark. Whilst the DSSC results for the new complexes **AS1-7** are somewhat not impressive, their preliminary efficiencies are remarkable in between the iridium based sensitisers. [13-16]

4. Conclusions

In this study, we synthesised and characterized seven new iridium (III)-based dyes with various aryltriazole cyclometalating ligands and dcb as anchoring ligand and they were preliminarily tested as sensitisers in TiO_2-based n-type dye-sensitised solar cells. The use of tandem Bestmann-

Ohira/CuAAC reaction in ligand design allows access to highly tunable ligand systems. Computational calculations were fundamental tools to design these new complexes and predict their proprieties. In line with expectations, the use of these phenyltriazole ligands led to a good spatial charge transfer directionality. The application of these complexes in unoptimized DSSC devices showed a reasonable photoelectrical response with efficiency up to 0.62%, the optimization of the singular cell component will definitely take to higher performances. The methodology reported here provides a potential route for facile tuning of photophysical and photovoltaic properties with greater ease than for existing ruthenium based systems. Future research will focus on improving on these initial studies and increasing the light absorbing properties of these dyes.

5. Acknowledgements

The authors wish to thank the Leverhulme Trust, The University of Huddersfield for funding this research. We also thank the Huddersfield High Performance Computing Research Group, the EPSRC and the national supercomputing service HECToR for computational resources utilised in this project.

Notes and reference

[1] B. O'Regan, M. Gratzel, Nature, 353 (1991) 737-740.

[2] L. Kavan, M. Gratzel, S.E. Gilbert, C. Klemenz, H.J. Scheel, J. Am. Chem. Soc., 118 (1996) 6716-6723.

[3] G.B. Hagfeldt, L. Sun, L. Kloo, H. Pettersson, Chem Rev, 110 (2010) 6595.

[4] M.K. Nazeeruddin, E. Baranoff, M. Grätzel, Solar Energy, 85 (2011) 1172.

[5] T. Bessho, E. Yoneda, J.-H. Yum, M. Guglielmi, I. Tavernelli, H. Imai, U. Rothlisberger, M.K. Nazeeruddin, M. Grätzel, J Am Chem Soc, 131 (2009) 5930-5934.

[6] K.-L. Wu, H.-C. Hsu, K. Chen, Y. Chi, M.-W. Chung, W.-H. Liu, P.-T. Chou, Chem Commun (Camb), 46 (2010) 5124-5126.

[7] S. Sinn, B. Schulze, C. Friebe, D.G. Brown, M. Jager, J. Kubel, B. Dietzek, C.P. Berlinguette, U.S. Schubert, Inorg Chem, 53 (2014) 1637-1645.

[8] P.G. Bomben, K.D. Thériault, C.P. Berlinguette, European Journal of Inorganic Chemistry, 2011 (2011) 1806-1814.

[9] T. Funaki, H. Funakoshi, O. Kitao, N. Onozawa-Komatsuzaki, K. Kasuga, K. Sayama, H. Sugihara, Angew Chem Int Ed Engl, 51 (2012) 7528-7531.

[10] A. Colombo, C. Dragonetti, A. Valore, C. Coluccini, N. Manfredi, A. Abbotto, Polyhedron, 82 (2014) 50-56.

[11] B. Happ, A. Winter, M.D. Hager, U.S. Schubert, Chem Soc Rev, 41 (2012) 2222-2255.
[12] E.I. Mayo, K. Kilsa, T. Tirrell, P.I. Djurovich, A. Tamayo, M.E. Thompson, N.S. Lewis, H.B. Gray, Photochem Photobiol Sci, 5 (2006) 871-873.
[13] A. Sinopoli, C.J. Wood, E.A. Gibson, P.I.P. Elliott, European Journal of Inorganic Chemistry, (2016) 2887-2890.
[14] E. Baranoff, J.-H. Yum, I. Jung, R. Vulcano, M. Grätzel, M.K. Nazeeruddin, Chem.-Asian J., 5 (2010) 496.
[15] E. Baranoff, J.-H. Yum, M. Graetzel, M.K. Nazeeruddin, Journal of Organometallic Chemistry, 694 (2009) 2661-2670.
[16] C. Dragonetti, A. Valore, A. Colombo, S. Righetto, V. Trifiletti, Inorganica Chimica Acta, 388 (2012) 163-167.
[17] F. Xu, H.U. Kim, J.-H. Kim, B.J. Jung, A.C. Grimsdale, D.-H. Hwang, Prog. Pol. Sci., 47 (2015) 92.
[18] K. Hasan, A.K. Bansal, I.D. Samuel, C. Roldan-Carmona, H.J. Bolink, E. Zysman-Colman, Sci. Rep., 5 (2015) 12325.
[19] K.P. Zanoni, R.L. Coppo, R.C. Amaral, N.Y. Murakami Iha, Dalton Trans, 44 (2015) 14559-14573.
[20] C. Lin, C. Xia, B. Ma, L. Zeng, A. Deangelis, E. Barron, in, Google Patents, 2012.
[21] B. Beyer, C. Ulbricht, D. Escudero, C. Friebe, A. Winter, L. González, U.S. Schubert, Organometallics, 28 (2009) 5478-5488.
[22] C. Ulbricht, B. Beyer, C. Friebe, A. Winter, U.S. Schubert, Adv Mater, 21 (2009) 4418-4441.
[23] P. Coppo, E.A. Plummer, L. De Cola, Chem Commun (Camb), (2004) 1774-1775.
[24] T.P. Lodge, Macromol., 42 (2009) 3827.
[25] V.V. Rostovtsev, L.G. Green, V.V. Fokin, K.B. Sharpless, Angew. Chem. Int. Ed., 41 (2002) 2596.
[26] M. Felici, P. Contreras-Carballada, J.M.M. Smits, R.J.M. Nolte, R.M. Williams, L.D. Cola, M.C. Feiters, Molecules, 15 (2010) 2039.
[27] B.S. Uppal, A. Zahid, P.I.P. Elliott, Eur. J. Inorg. Chem., 2013 (2013) 2571.
[28] A. R.Oki, R.J. Morgan, Synt. Commun., 25 (1995) 4093.
[29] D. Luvino, Synlett, 19 (2007) 3037.
[30] M. Valiev, E.J. Bylaska, N. Govind, K. Kowalski, T.P. Straatsma, H.J.J.V. Dam, D. Wang, J. Nieplocha, E. Apra, T.L. Windus, W.d. Jong, Comp. Phys. Commun., 181 (2010) 1477.
[31] P.J. Stephens, F.J. Devlin, C.F. Chabalowski, M.J. Frisch, J. Phys. Chem., 98 (1994) 11623.
[32] D. Andrae, U. Haussermann, M. Dolg, H. Stoll, H. Preuss, Theor. Chim. Acta, 77 (1990) 123.
[33] A. Klamt, Wiley Interdisciplinary Reviews: Computational Molecular Science, 1 (2011) 699-709.

[34] S. Lamansky, P. Djurovich, D. Murphy, F. Abdel-Razzaq, H-E Lee, C. Adachi, P.E. Burrows, S.R. Forrest, M.E. Thompson, J. Am. Chem. Soc., 123 (2001) 4304.

[35] A.B. Tamayo, S. Garon, T. Sajoto, P.I. Djurovich, I.M. Tsyba, R. Bau, M.E. Thompson, Inorg Chem, 44 (2005) 8723-8732.

[36] S. Bettington, M. Tavasli, M.R. Bryce, A. Beeby, H. Al-Attar, A.P. Monkman, Chemistry, 13 (2007) 1423-1431.

[37] C.-H. Yang, S.-W. Li, Y. Chi, Y.-M. Cheng, Y.-S. Yeh, P.-T. Chou, G.-H. Lee, C.-H. Wang, C.-F. Shu, Inorg Chem, 44 (2005) 7770-7780.